

# Noise Characterization in Cine DENSE MRI

D. Kim<sup>1</sup> and P. Kellman<sup>2</sup>

<sup>1</sup>Radiology, New York University, New York, New York, United States, <sup>2</sup>NIH-NHLBI-LCE, Maryland, United States

**Introduction:** Cine displacement-encoded (DENSE) MRI [1] is a high spatial resolution modality for the quantification of intramyocardial function. The noise in phase contrast MRI has been characterized as inversely proportional to the magnitude of magnetization [2]. In DENSE MRI, however, the calculation of the strain involves more complex processes, including a finite element model; the propagation of phase errors to the calculation of strain is less straight forward [3,4]. In echo-combined DENSE MRI, the intrinsic phase correction does not eliminate the systematic error due static magnetic field inhomogeneity ( $B_0$ ), because the two echoes being combined are separated by a time interval. As such, the residual phase error term is equal to  $\Delta F \Delta T$ , where  $\Delta F$  is the off-resonant frequency and  $\Delta T$  is the time interval between each echo and TE, as previously described [4]. The purpose of this study, therefore, was to empirically characterize the relative contribution of the systematic and random noise to displacement and strain maps in cine DENSE MRI as a function of signal-to-noise ratio (SNR) and  $B_0$  variation.

**Methods:** The cine DENSE pulse sequence using balanced steady state of free precession (b-SSFP) readouts, echo-combination reconstruction [4,5,6] and temporal sensitivity encoding (TSENSE)[4,7] parallel imaging reconstruction was implemented on a 3T whole-body MR scanner (Tim Trio; Siemens). Imaging parameters included: field of view = 320 x 320 mm, acquisition matrix = 192 x 72, slice thickness = 7 mm, TE/TR = 1.47/2.93 ms, bandwidth = 744 Hz/pixel, acceleration factor = 2, phase-encoding lines per cardiac phase per cardiac cycle = 12, cardiac phases = 22, and temporal resolution = 35 ms. The acquisition time for each multi-phase DENSE data was 3 heartbeats, and the total acquisition time to acquire two orthogonal sets of two complementary DENSE image sets was 12 heartbeats, as previously described [4]. Image acquisition was repeated using six different flip angles (1°, 2°, 5°, 10°, 15°, and 20°) to achieve a wide range of SNR. Displacement was encoded on the phase of the magnetization using 1-1 spatial modulation of magnetization pulses with gradient encoding strength of 0.94 radians/mm. The stationary phantom imaging experiment was performed with simulated electrocardiogram at 60 beats per minute and with altered shim currents to emulate the 130Hz peak-to-peak  $B_0$  variation in the heart at 3T [8]. The agarose gel phantom had relaxation times ( $T_1 \approx 1100$  ms and  $T_2 \approx 40$  ms) which are comparable to those of the myocardium at 3T. For image analysis, the displacement, first principle strain ( $E_1$ ) and second principle strain ( $E_2$ ) values were calculated from the echo-combined phase data as previously described [4,5]. The root-mean-square (RMS) values were calculated for the multi-phase displacement,  $E_1$ , and  $E_2$  maps. The multiple flip angle data points were pooled, and the RMS of displacement,  $E_1$ , and  $E_2$  values were plotted as a function of SNR. Using the same phase data sets of six flip angles, the displacement and strain calculations were repeated with the original phase values multiplied by the factors 1Hz/130Hz and 70Hz/130Hz, in order to emulate an excellent shimming condition and the  $B_0$  variation of 70Hz in the heart at 1.5T [9], respectively. Note the latter condition is equivalent to the combination of  $B_0$  variation of 130Hz in the heart at 3T and bandwidth = 1382 Hz/pixel.

**Results:** Figure 1 shows representative  $E_2$  error maps for four conditions: 1) SNR = 40 and  $\Delta B_0 = 130$ Hz, 2) SNR = 23 and  $\Delta B_0 = 130$ Hz, 3) SNR = 40 and  $\Delta B_0 = 70$ Hz, and 4) SNR = 23 and  $\Delta B_0 = 70$ Hz. Note that the  $E_2$  maps at conditions 2 and 4 appear similar. Figure 2 shows plots of RMS of displacement,  $E_1$ , and  $E_2$  as a function of SNR and  $\Delta B_0$ . In the displacement map, the systematic error dominated over the random noise for SNR > 10, suggesting that SNR >10 does not further reduce the displacement error. In the  $E_1$  map, the systematic error dominated over the random noise for SNR >20, but  $E_1$  continued to decrease at a slow rate as a function of SNR. In the  $E_2$  map, both the systematic error and random noise contributed to the error, and  $E_2$  converged at SNR = 60.

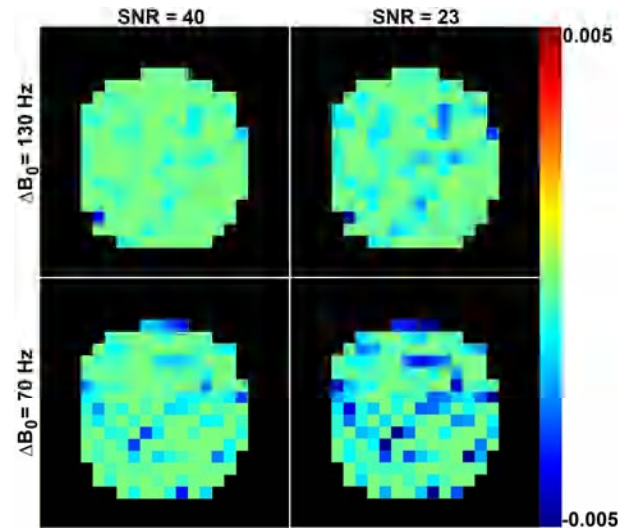


**Fig. 1.** Representative  $E_2$  error maps: (upper left) SNR=40 and  $\Delta B_0 = 130$ Hz, (upper right) SNR=23 and  $\Delta B_0 = 130$ Hz, (lower left) SNR = 40 and  $\Delta B_0 = 70$  Hz, and (lower right) SNR =23 and  $\Delta B_0 = 70$  Hz.

Figure 2 shows plots of RMS of displacement,  $E_1$ , and  $E_2$  as a function of SNR and  $\Delta B_0$ . In the displacement map, the systematic error dominated over the random noise for SNR > 10, suggesting that SNR >10 does not further reduce the displacement error. In the  $E_1$  map, the systematic error dominated over the random noise for SNR >20, but  $E_1$  continued to decrease at a slow rate as a function of SNR. In the  $E_2$  map, both the systematic error and random noise contributed to the error, and  $E_2$  converged at SNR = 60.

**Discussion:** This study has characterized the relative contribution of systematic and random noise to the displacement,  $E_1$ , and  $E_2$  error maps in cine DENSE MRI using b-SSFP readouts, echo-combination reconstruction, and TSENSE parallel imaging. Our previous work has shown that this pulse sequence at 3T can achieve myocardial SNR ranging from 30-10 (early diastole - late diastole)[4]. Assuming end-systolic control displacement,  $E_1$ , and  $E_2$  values of 5 mm, 0.4, and -0.2, respectively, and assuming a 95% confidence interval, the acceptable displacement,  $E_1$ , and  $E_2$  error values are 0.25 mm, 0.02, and 0.01, respectively. These results show that the displacement,  $E_1$ , and  $E_2$  errors were within the aforementioned acceptable ranges. Compared to the  $E_2$  map, both the displacement and  $E_1$  maps were comparatively improved less by increasing the SNR > 20, suggesting that  $E_2$  maps are comparatively more sensitive to the random noise. Two approaches to further reduce the systematic error are performing effective shimming and acquiring the data with higher receiver bandwidth, but the latter also increases the random noise.

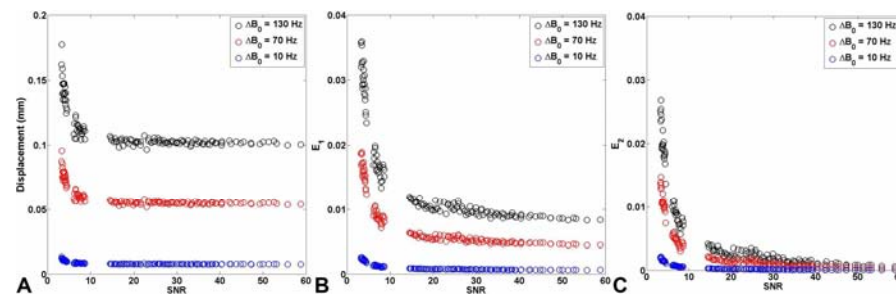


**Fig. 2.** Plots of RMS of (A) displacement, (B)  $E_1$ , and (C)  $E_2$  as a function of SNR and  $B_0$ .

## References

1. Kim, D et al. Radiology 2004; 230:862-871.
2. Bernstein, MA et al. MRM 1994; 32: 330-334.
3. Aletras, AH et al. JMR 2005: 176:99-106.
4. Kim, D et al. NMR Biomed (in press).
5. Kim, D et al. MRM 2004; 52:188-192.
6. Ryf, S et al. JMRI 2004; 20: 874-880.
7. Kellman, P et al. MRM 2001; 45:846-852.
8. Noeske, R et al. MRM 2000: 44:978-982.
9. Reeder, SB et al. MRM 1998: 39:988-998.